

A tensor formalism for multilayer network centrality measures using the Einstein product

Smahane El-Halouy^a, Silvia Noschese^b, Lothar Reichel^c

^a*Department of Mathematical Sciences, Kent State University, Kent, OH 44242, USA, and Laboratory LAMAI, Faculty of Sciences and Technologies, Cadi Ayyad University, Marrakech, Morocco.*

^b*Dipartimento di Matematica “Guido Castelnuovo”, SAPIENZA Università di Roma, P.le A. Moro, 2, I-00185 Roma, Italy.*

^c*Department of Mathematical Sciences, Kent State University, Kent, OH 44242, USA.*

Abstract

Complex systems that consist of diverse kinds of entities that interact in different ways can be modeled by multilayer networks. This paper uses the tensor formalism with the Einstein product to model this type of networks. Several centrality measures, that are well known for single-layer networks, are extended to multilayer networks using tensors and their properties are investigated. In particular, subgraph centrality based on the exponential and resolvent of a tensor are considered. Krylov subspace methods based on the tensor format are introduced for computing approximations of different measures for large multilayer networks.

Keywords: multilayer networks, centrality measures, adjacency tensor, tensor functions, Einstein product, Krylov subspace method

2010 MSC: 05C50, 15A18, 65F15

1. Introduction

A network is a set of objects that are connected to each other in some fashion. Mathematically, a *single-layer network* is represented by a graph $G = \{V, E\}$, where the elements of the set $V = \{v_i\}_{i=1}^n$, referred to as vertices or nodes, represent the objects, and the elements of the set $E \subseteq V \times V$, designated as edges, represent the connections between the nodes. We denote an edge from node v_i to node v_j by $v_i \rightarrow v_j$.

Some real world examples require the modeling of more than one kind of nodes or of more than one type of edges. This holds, for instance, for the transportation network in a country when considering different means of transportation. The train and bus routes are different types of connections and should in

Email addresses: elhalouysmahane@gmail.com (Smahane El-Halouy), noschese@mat.uniroma1.it (Silvia Noschese), reichel@math.kent.edu (Lothar Reichel)

some models be represented by different kinds of edges. Moreover, train and bus stations may make up nodes with diverse properties. The connections between a train station and an adjacent bus station give rise to yet another kind of edges connecting different kinds of nodes, along which travelers typically walk. This kind of objects and connections can be modeled by *multilayer networks*, which emphasize different kinds or connections, known as layers, between possibly different kinds of elements of a network. Each layer is represented by a single graph that contains the elements, or some of the elements, of the network and the connections between them in this layer. Edges connecting nodes from different layers model the interactions between different layers. Therefore, the nodes in a multilayer network require two indices, e.g., v_i^ℓ , where the superscript ℓ denotes the layer, and the subscript i determines the node in this layer. The set $V_L = V \times L$ represents all possible combinations of node-layers, where the set V is made up of all nodes of the network considered. Each layer may be made up of V or some elements of V , and L is the set of layers. The set of edges $E \subseteq V_L \times V_L$ represents all edges of the network. The special case when the set of nodes is the same in all layers, and edges that connect nodes in different layers are only allowed between a node and its copy in another layer, is known as a *multiplex network*. A nice recent paper by Bergermann and Stoll [7] studies multiplex networks and generalized matrix function-based centrality measures to this kind of networks. The authors use supra-adjacency matrices to represent multiplex networks. Recently, a global measure of communicability in a multiplex network, computed by means of the Perron root, and the right and left Perron vectors of the supra-adjacency matrix associated with this kind of network was introduced in [16]. We are interested in using tensors for network analysis, because they arise naturally when modeling multilayer networks.

The model mentioned above can be generalized to represent not only networks with multiple layers but also different aspects. To allow for the modeling of more than one aspect, we define a sequence $\{L_j\}_{j=1}^d$ of sets of elementary layers with d being the number of aspects that we would like to model; L_j is the set of layers for aspect j . Then the total number of layers is $|L_1| \times |L_2| \times \dots \times |L_d|$ and we have $V_L = V \times L_1 \times \dots \times L_d$. The nodes now are identified by using $d+1$ indices $v_i^{\ell_1, \dots, \ell_d}$, where the subscript i indicates the number of the node and the superscript ℓ_1, \dots, ℓ_d shows the specific layer. For more details on this kind of generalization, we refer to [12, 30] and the references therein, where general frameworks for multilayer network are discussed together with their mathematical formulation. Figure 1 illustrates a simple multilayer network with 2 aspects; this figure can also be found in [9]. An example of a real multilayer network with multiple aspects in biology is provided in [32], where the first aspect is the type of data (genomic, metabolomic, or proteomic), and the second aspect models different biological pathways; see Figure 2 in [32].

Single-layer networks are often represented by an adjacency matrix, which is helpful for extracting information about the network, e.g, by evaluating functions of the the adjacency matrix or by computing certain eigenvectors of this matrix. For instance, Estrada and Higham [20] describe how the matrix exponential and resolvent can be used to determine how easy it is to communi-

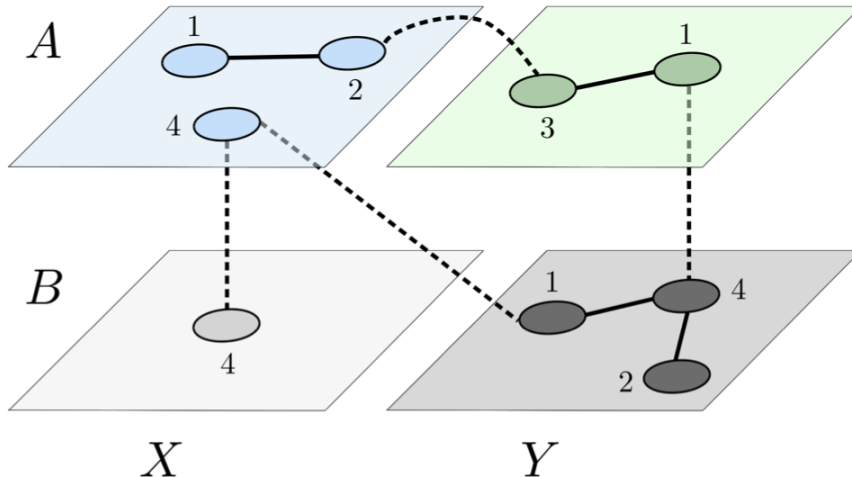


Figure 1: An example of a multilayer network with a set of four nodes $V = \{1, 2, 3, 4\}$ and two aspects, the corresponding elementary layer sets $L_1 = \{A, B\}$ and $L_2 = \{X, Y\}$. The total number of layers is four and they are (A, X) , (A, Y) , (B, X) and (B, Y) . Each layer includes some of the elements of V .

cate between nodes in a single-layer network, and which nodes are the most important ones; see also Estrada [18] and references therein. For multilayer networks, we use tensors, i.e., a multidimensional generalization of matrices, and represent the network by a $2(d+1)$ -order adjacency tensor \mathcal{A} of size $(|V| \times |L_1| \times \dots \times |L_d|) \times (|V| \times |L_1| \times \dots \times |L_d|)$, where $|V|$ denotes the total number of nodes, and $|L_j|$ designates the number of layers for property j , for $j = 1, 2, \dots, d$. The entry $\mathcal{A}(i, \ell_1, \dots, \ell_d, j, k_1, \dots, k_d)$ of the tensor \mathcal{A} for an *unweighted* multilayer network with sets of layers L_j , $j = 1, 2, \dots, d$, is one if there is an edge $v_i^{\ell_1, \dots, \ell_d} \rightarrow v_j^{k_1, \dots, k_d}$; otherwise the tensor entry is zero. For a *weighted* network a tensor entry 1 may be replaced by a real, generally positive, number. In a directed network some of the edges represent “one-way streets”. Note that some nodes may not be present in all layers. Therefore, considering empty nodes is necessary to allow the tensorial representation. For instance, the network illustrated in Figure 1 can be represented by a 6^{th} order tensor of size $4 \times 2 \times 2 \times 4 \times 2 \times 2$ by adding empty nodes so that every layer is made up of 4 nodes.

Adjacency tensors allow us to capture the structure and complexity of relationships between the nodes of a multilayer network. We are interested in investigating and generalizing some centrality measures that are well established for single-layer networks to multilayer networks by using the tensor formalism and applying tensor tools, such as the Einstein product and tensor functions. Several centrality measures have been studied for multilayer networks using the

tensor formalism in [13]. Eigenvector multicentrality has been investigated for multilayer networks via a tensor-based framework in [35]; see also [11]. In addition to generalizing centrality measures that are commonly used for single-layer networks to multilayer networks, we describe practical and efficient ways to compute these measures by using Krylov subspace methods based on the tensor format.

This paper is organized as follows. Tensor notation, definitions, and properties used throughout this paper are described in Section 2. Section 3 discusses the extension of matrix functions to tensor functions using the Einstein tensor product. We define centrality measures for multilayer networks based on the tensor representation and tensor functions. Section 4 describes Krylov subspace methods based on the tensor format using the Einstein product, and discusses their application to the approximation of tensor functions. Section 5 presents a few computed examples and Section 6 contains concluding remarks.

2. Preliminaries

This section presents notation and properties of tensors that will be used throughout this paper. We start with a generalization of the matrix-matrix product to tensors that is referred to as the Einstein product.

Definition 1 (Einstein Product). Let $\mathcal{A} \in \mathbb{R}^{I_1 \times \dots \times I_N \times J_1 \times \dots \times J_M}$ and $\mathcal{B} \in \mathbb{R}^{J_1 \times \dots \times J_M \times K_1 \times \dots \times K_L}$ be tensors of orders $N+M$ and $M+L$, respectively. The product $\mathcal{C} = \mathcal{A} *_M \mathcal{B} \in \mathbb{R}^{I_1 \times \dots \times I_N \times K_1 \times \dots \times K_L}$ of the tensors \mathcal{A} and \mathcal{B} is a tensor of order $N+L$ with entries

$$\mathcal{C}_{i_1, \dots, i_N, k_1, \dots, k_L} = \sum_{j_1, \dots, j_M} \mathcal{A}_{i_1, \dots, i_N, j_1, \dots, j_M} \mathcal{B}_{j_1, \dots, j_M, k_1, \dots, k_L}.$$

It is commonly referred to as the Einstein product; see [8, 10, 15]. The subscript M in $*_M$ indicates the last and first M dimensions of \mathcal{A} and \mathcal{B} , respectively, over which the sum is evaluated.

The identity tensor $\mathcal{I} = [\mathcal{I}_{i_1, \dots, i_N, j_1, \dots, j_N}] \in \mathbb{R}^{I_1 \times \dots \times I_N \times I_1 \times \dots \times I_N}$ under the Einstein product has the entries

$$\mathcal{I}_{i_1, \dots, i_N, j_1, \dots, j_N} = \begin{cases} 1, & \text{if } i_k = j_k, \text{ for } k = 1, 2, \dots, N, \\ 0, & \text{otherwise.} \end{cases}$$

Remark 1. A tensor of even order $\mathcal{A} \in \mathbb{R}^{I_1 \times \dots \times I_N \times J_1 \times \dots \times J_N}$ is said to be square if the first set of dimensions equals the second set, i.e., if $I_k = J_k$ for $k = 1, 2, \dots, N$; see, e.g., [33]. The adjacency tensor of a multilayer network is of even order and square, however, for some computations tensors of different orders are required. This is possible when using the Einstein product by choosing a suitable number of dimensions over which we carry out the summation.

Remark 2. The transpose of a tensor $\mathcal{A} \in \mathbb{R}^{I_1 \times \dots \times I_N \times J_1 \times \dots \times J_M}$ is a tensor $\mathcal{B} \in \mathbb{R}^{J_1 \times \dots \times J_M \times I_1 \times \dots \times I_N}$ such that $\mathcal{A}_{i_1, \dots, i_N, j_1, \dots, j_M} = \mathcal{B}_{j_1, \dots, j_M, i_1, \dots, i_N}$; see, e.g., [33].

The n -mode product is a well-known tensor-matrix product; see [29]. For an N^{th} order tensor $\mathcal{A} \in \mathbb{R}^{I_1 \times \dots \times I_N}$ and a matrix $A \in \mathbb{R}^{I_n \times J}$, their n -mode product is an N^{th} order tensor $\mathcal{A} \times_n A \in \mathbb{R}^{I_1 \times \dots \times I_{n-1} \times J \times I_{n+1} \times \dots \times I_N}$.

If $\mathcal{A} \in \mathbb{R}^{I_1 \times \dots \times I_N \times J}$ is an $(N+1)^{\text{th}}$ order tensor and $A \in \mathbb{R}^{J \times I}$, then the n -mode product of \mathcal{A} and A over mode $N+1$ is the same as the Einstein product when summing over the last mode of the tensor. In other words, we have

$$\mathcal{A} *_1 A = \mathcal{A} \times_{N+1} A^T.$$

We can reorganize the entries of a tensor in different ways to obtain a 2D array, i.e., a matrix. This transformation is known as *matricization* or *flattening*. We flatten a tensor by using lexicographical ordering of the indices.

Definition 2 (Tensor flattening). Let $\mathcal{A} \in \mathbb{R}^{I_1 \times \dots \times I_N \times J_1 \times \dots \times J_M}$ be a tensor of order $N+M$. The elements of the matrix $A \in \mathbb{R}^{I_1 \dots I_N \times J_1 \dots J_M}$ obtained by flattening the tensor \mathcal{A} are given by

$$A_{i,j} = \mathcal{A}_{i_1, \dots, i_N, j_1, \dots, j_M},$$

where

$$\begin{aligned} i &= i_1 + \sum_{p=2}^N (i_p - 1) \prod_{q=1}^{p-1} I_q, \\ j &= j_1 + \sum_{p=2}^M (j_p - 1) \prod_{q=1}^{p-1} J_q. \end{aligned}$$

Here and below the indices i_p and j_p live in their domains, i.e., $1 \leq i_p \leq I_p$ for $1 \leq p \leq N$, and $1 \leq j_q \leq J_q$ for $1 \leq q \leq M$. We define $A = \text{mat}(\mathcal{A})$ and $\mathcal{A} = \text{mat}^{-1}(A)$.

Remark 3. For a multiplex network, $\text{mat}(\mathcal{A})$ is the supra-adjacency matrix defined in [7].

Proposition 1. Let $\mathcal{A} \in \mathbb{R}^{I_1 \times \dots \times I_N \times J_1 \times \dots \times J_M}$ and $\mathcal{B} \in \mathbb{R}^{J_1 \times \dots \times J_M \times K_1 \times \dots \times K_L}$ be tensors of orders $N+M$ and $M+L$, respectively. Then

$$\text{mat}(\mathcal{A} *_M \mathcal{B}) = \text{mat}(\mathcal{A}) \cdot \text{mat}(\mathcal{B}),$$

where \cdot denotes the usual matrix product.

Proof: The result follows by direct computations; see [10] for details. \square

Definition 3. The following definitions can be found in, e.g., [10, 28, 33].

1. The trace of a square tensor, $\mathcal{A} \in \mathbb{R}^{I_1 \times \dots \times I_N \times I_1 \times \dots \times I_N}$, is given by

$$\text{tr}(\mathcal{A}) = \sum_{i_1, \dots, i_N} \mathcal{A}_{i_1, \dots, i_N, i_1, \dots, i_N}.$$

2. The inner product of two tensors of the same size $\mathcal{X}, \mathcal{Y} \in \mathbb{R}^{I_1 \times \dots \times I_N \times J_1 \times \dots \times J_M}$ is defined as

$$\langle \mathcal{X}, \mathcal{Y} \rangle = \sum_{i_1, \dots, i_N, j_1, \dots, j_M} \mathcal{X}_{i_1, \dots, i_N, j_1, \dots, j_M} \mathcal{Y}_{i_1, \dots, i_N, j_1, \dots, j_M}.$$

For square tensors, we have

$$\langle \mathcal{X}, \mathcal{Y} \rangle = \text{tr}(\mathcal{X}^T *_N \mathcal{Y}).$$

3. The Frobenius norm of a tensor is given by

$$\|\mathcal{X}\|_F = \sqrt{\langle \mathcal{X}, \mathcal{X} \rangle}.$$

If \mathcal{X} is a square tensor, then

$$\|\mathcal{X}\|_F = \sqrt{\text{tr}(\mathcal{X}^T *_N \mathcal{X})}.$$

4. For a positive integer p , we define the p^{th} power of a square tensor $\mathcal{A} \in \mathbb{R}^{I_1 \times \dots \times I_N \times I_1 \times \dots \times I_N}$ by using the Einstein product recursively as

$$\mathcal{A}^p = \mathcal{A} *_N \mathcal{A}^{p-1},$$

where $\mathcal{A}^0 = \mathcal{I}$ is the identity tensor.

Proposition 2. One has

$$\|\mathcal{A}\|_F = \|\text{mat}(\mathcal{A})\|_F \tag{1}$$

and, if \mathcal{A} is a square tensor, then

$$\|\mathcal{A}^p\|_F \leq \|\mathcal{A}\|_F^p. \tag{2}$$

Proof: Let $\mathcal{A} \in \mathbb{R}^{I_1 \times \dots \times I_N \times J_1 \times \dots \times J_M}$ be a tensor of order $N + M$. One has

$$\|\mathcal{A}\|_F = \sqrt{\langle \mathcal{A}, \mathcal{A} \rangle} = \sqrt{\sum_{i_1, \dots, i_N, j_1, \dots, j_M} \mathcal{A}_{i_1, \dots, i_N, j_1, \dots, j_M}^2} = \sqrt{\sum_{i=1}^N \sum_{j=1}^M A_{i,j}^2} = \|A\|_F,$$

with $A = \text{mat}(\mathcal{A})$ given in Definition 2. This shows (1). Assume now that $M = N$. According to Definition 3(4.), by applying Proposition 1 $p - 1$ times, one has $\text{mat}(\mathcal{A}^p) = (\text{mat}(\mathcal{A}))^p$, so that $\|\text{mat}(\mathcal{A}^p)\|_F \leq \|\text{mat}(\mathcal{A})\|_F^p$, where the inequality is due to the submultiplicativity of the Frobenius matrix norm. Thus, thanks to (1), one has inequality (2). \square

Remark 4. The eigenvalue problem for 4th-order tensors is discussed in [12]. We can express this problem for any square tensor by using the Einstein product; we have

$$\mathcal{A} *_N \mathcal{X} = \lambda \mathcal{X},$$

where $\mathcal{A} \in \mathbb{R}^{I_1 \times \dots \times I_N \times I_1 \times \dots \times I_N}$, $\mathcal{X} \in \mathbb{R}^{I_1 \times \dots \times I_N}$ and $\lambda \in \mathbb{C}$. This eigenvalue problem is equivalent to the matrix eigenvalue problem $\text{mat}(\mathcal{A}) \cdot \text{vec}(\mathcal{X}) = \lambda \text{vec}(\mathcal{X})$, where vec is the vectorization operator that takes a tensor and rearranges it into a single column vector by concatenating its elements, i.e., it stacks the elements \mathcal{X} to form a column vector.

3. Tensor functions and centrality measures for multilayer networks

Centrality measures have been thoroughly studied for single-layer networks. These measures include Katz centrality, subgraph centrality, and total communicability with respect to a node; see, e.g., [5, 14, 18, 19, 20, 21]. In this section, we introduce analogues of these measures for multilayer networks using the adjacency tensor and the Einstein product.

We recall that, for single-layer networks, a walk from node v_{i_1} to node v_{i_j} is defined as a sequence of edges

$$v_{i_1} \rightarrow v_{i_2}, v_{i_2} \rightarrow v_{i_3}, \dots, v_{i_{j-1}} \rightarrow v_{i_j}$$

that can be traversed to reach node v_{i_j} from node v_{i_1} . The length of the walk is the number of edges, $j - 1$. Nodes and edges may be repeated in a walk. A walk is said to be short if $j - 1$ is fairly small. There may be an edge from node i in layer $(\ell_1, \ell_2, \dots, \ell_d)$ to node j in layer (k_1, k_2, \dots, k_d) in a multilayer network. We denote this edge by $v_i^{\ell_1, \ell_2, \dots, \ell_d} \rightarrow v_j^{k_1, k_2, \dots, k_d}$. A walk in a multilayer network from node $v_{i_1}^{\ell_{k_1}, \dots, \ell_{k_d}}$ to node $v_{i_j}^{\ell_{k_1+j}, \dots, \ell_{k_d+j}}$ is defined as a sequence of edges such as

$$\begin{aligned} v_{i_1}^{\ell_{k_1}, \dots, \ell_{k_d}} &\rightarrow v_{i_2}^{\ell_{k_1+1}, \dots, \ell_{k_d+1}}, & v_{i_2}^{\ell_{k_1+1}, \dots, \ell_{k_d+1}} &\rightarrow v_{i_3}^{\ell_{k_1+2}, \dots, \ell_{k_d+2}}, \dots, \\ v_{i_{j-1}}^{\ell_{k_1+j-1}, \dots, \ell_{k_d+j-1}} &\rightarrow v_{i_j}^{\ell_{k_1+j}, \dots, \ell_{k_d+j}} \end{aligned}$$

that can be traversed to reach node $v_{i_j}^{\ell_{k_1+j}, \dots, \ell_{k_d+j}}$ from node $v_{i_1}^{\ell_{k_1}, \dots, \ell_{k_d}}$. The length of the walk is the number of edges, $j - 1$, and nodes and edges may be repeated in a walk. A closed multilayer walk is a multilayer walk for which the starting and ending nodes are the same, i.e., $i_1 = i_j$ and $\ell_{k_n} = \ell_{k_n+j}$, for $n = 1, 2, \dots, d$. Estrada [17] has defined a walk in a multiplex network in an analogous fashion.

The entries of the adjacency tensor $\mathcal{A} \in \mathbb{R}^{N \times K_1 \times \dots \times K_d \times N \times K_1 \times \dots \times K_d}$ of an unweighted undirected multilayer network tell us whether there is an edge between any pair of nodes (between the same or different layers). The entries of the Einstein product of the adjacency tensor \mathcal{A} with itself,

$$\begin{aligned} \mathcal{B}_{i, \ell_1, \ell_2, \dots, \ell_d, j, k_1, k_2, \dots, k_d} &= \mathcal{A} *_d \mathcal{A} \\ &= \sum_{p, q_1, \dots, q_d} \mathcal{A}_{i, \ell_1, \ell_2, \dots, \ell_d, p, q_1, \dots, q_d} \mathcal{A}_{p, q_1, \dots, q_d, j, k_1, k_2, \dots, k_d}, \end{aligned}$$

where $1 \leq i, j \leq N$, $1 \leq \ell_s, k_s \leq L$, $1 \leq s \leq d$, show the number of multilayer walks of length 2 between pairs of nodes $v_i^{\ell_1, \ell_2, \dots, \ell_d}$ and $v_j^{k_1, k_2, \dots, k_d}$. Similarly, let p be a positive integer. Then the entries of the tensor $\mathcal{A}^p = \mathcal{A} *_{d+1} \mathcal{A}^{p-1}$ display the number of multilayer walks of length p between pairs of nodes $v_i^{\ell_1, \ell_2, \dots, \ell_d}$ and $v_j^{k_1, k_2, \dots, k_d}$. In addition, the entry $\mathcal{A}_{i, \ell_1, \ell_2, \dots, \ell_d, i, \ell_1, \ell_2, \dots, \ell_d}^p$ provides the number of closed multilayer walks of length p that start at node $v_i^{\ell_1, \ell_2, \dots, \ell_d}$. This suggests, in order to take into account walks of all possible lengths $p \geq 0$, the introduction of the tensor function

$$f(\mathcal{A}) = \sum_{p=0}^{\infty} c_p \mathcal{A}^p, \quad (3)$$

where the coefficients c_p generally are real and nonnegative, and are chosen so that the series converges.

Let the tensor $\mathcal{E}_{s, t_1, \dots, t_d} \in \mathbb{R}^{N \times K_1 \times \dots \times K_d}$ with all entries equal to zero except for the $(s, t_1, \dots, t_d)^{\text{th}}$ entry, which is one. We refer to the entry

$$f(\mathcal{A})_{i, \ell_1, \ell_2, \dots, \ell_d, j, k_1, k_2, \dots, k_d} = \mathcal{E}_{i, \ell_1, \ell_2, \dots, \ell_d} *_{d+1} f(\mathcal{A}) *_{d+1} \mathcal{E}_{j, k_1, k_2, \dots, k_d} \quad (4)$$

as the *communicability* from node $v_i^{\ell_1, \ell_2, \dots, \ell_d}$ to node $v_j^{k_1, k_2, \dots, k_d}$; a relatively large value indicates that it is easy to send information from node $v_i^{\ell_1, \ell_2, \dots, \ell_d}$ to node $v_j^{k_1, k_2, \dots, k_d}$. Moreover, we refer to the entry

$$f(\mathcal{A})_{i, \ell_1, \ell_2, \dots, \ell_d, i, \ell_1, \ell_2, \dots, \ell_d} = \mathcal{E}_{i, \ell_1, \ell_2, \dots, \ell_d} *_{d+1} f(\mathcal{A}) *_{d+1} \mathcal{E}_{i, \ell_1, \ell_2, \dots, \ell_d} \quad (5)$$

as the *subgraph centrality* of node $v_i^{\ell_1, \ell_2, \dots, \ell_d}$; a relatively large value indicates that this node is important because much information may pass through it. These notions of communicability and subgraph centrality for nodes in multilayer graphs generalize the analogous definitions introduced and explored by Estrada and his collaborators, as well as others, in [1, 14, 19, 20, 21] for single-layer networks. In these references \mathcal{A} in (3) is replaced by the adjacency matrix for the single-layer graph and, hence, f is a matrix function.

In many network applications short walks are more important than long walks, because it is easier to transmit information via a few edges than via many edges. This suggests that the coefficients c_p should satisfy $0 \leq c_{p+1} \leq c_p$ for large p -values. One of the most commonly used matrix functions for single-layer networks is the matrix exponential. For multilayer networks, we therefore introduce the tensor exponential

$$\exp(\beta \mathcal{A}) = \sum_{p=0}^{\infty} \frac{\beta^p \mathcal{A}^p}{p!}.$$

It follows from Propositions 1 and 2 that this series converges for any fixed β in the interval $0 \leq \beta < \infty$. Since the first term \mathcal{I} has no natural interpretation in the context of network modeling, we will use the modified tensor exponential

$$\exp_0(\beta \mathcal{A}) := \exp(\beta \mathcal{A}) - \mathcal{I}, \quad (6)$$

where \mathcal{I} denotes the identity tensor.

We introduce the δ -effective diameter of the network determined by the tensor function (3). It is defined as the smallest integer k such that

$$\frac{\max_{\ell > k} |c_\ell|}{\max_{1 \leq j \leq k} |c_j|} \leq \delta, \quad (7)$$

for some small $\delta > 0$. Roughly, this diameter is k if the tensor function (3) can be approximated well by a polynomial of degree k . This means that walks of length larger than k do not significantly affect the properties of the network. for some small $\delta > 0$. Its importance for the communicability in single-layer networks is explored in [1]. The definition of the effective diameter in [1] differs slightly from (7) and is for matrix functions.

Proposition 3. *Let the tensor function (3) be the modified tensor exponential (6) for some $\beta > 0$. Then the left-hand side of (7) decreases to zero as k increases.*

Proof: Assume that $\beta > 1$ and let k_β denote the integer part of β . Then

$$\max_{\ell > k} c_\ell = \begin{cases} \frac{\beta^{k_\beta}}{k_\beta!} & \text{if } k < k_\beta, \\ \frac{\beta^{k+1}}{(k+1)!} & \text{if } k \geq k_\beta, \end{cases}$$

and

$$\max_{1 \leq j \leq k} c_j = \begin{cases} \frac{\beta^{k_\beta}}{k_\beta!} & \text{if } k \geq k_\beta, \\ \frac{\beta^k}{k!} & \text{if } k < k_\beta. \end{cases}$$

It follows that

$$\frac{\max_{\ell > k} c_\ell}{\max_{1 \leq j \leq k} c_j} = \begin{cases} \frac{\beta^{k_\beta}}{k_\beta!} \cdot \frac{k!}{\beta^k} & \text{if } k < k_\beta, \\ \frac{\beta^{k+1}}{(k+1)!} \cdot \frac{k_\beta!}{\beta^{k_\beta}} & \text{if } k \geq k_\beta. \end{cases}$$

Therefore this quotient converges to zero as k increases.

We turn to the situation when $0 < \beta \leq 1$. Then $\max_{1 \leq j \leq k} c_j = c_1$ and

$$\max_{\ell > k} c_\ell = c_{k+1} = \frac{\beta^{k+1}}{(k+1)!} \rightarrow 0 \text{ as } k \rightarrow \infty,$$

and the proposition follows. \square

Resolvents of the adjacency matrix also are commonly used to determine properties of nodes in a single-layer network; see, e.g., Estrada and Higham [20] and Katz [27]. We define the modified tensor resolvent,

$$\text{res}_0(\mathcal{A}, \alpha) = (\mathcal{I} - \alpha \mathcal{A})^{-1} - \mathcal{I} = \sum_{p=1}^{\infty} \alpha^p \mathcal{A}^p, \quad (8)$$

which is convergent for $0 < \alpha < 1/|\lambda_{\max}|$, where λ_{\max} denotes an eigenvalue of largest magnitude of \mathcal{A} . For many adjacency tensors of interest, λ_{\max} is real and positive. Conditions under which this is the case are discussed by Qi and Luo [33]. The eigenvalue λ_{\max} can be computed as an eigenvalue of a matrix using the relation of Remark 4. The choice of α affects the δ -effective diameter of the tensor function (8). This is discussed for the matrix resolvent in [1].

We also define the *multilayer total communicability of node* $v_i^{\ell_1, \ell_2, \dots, \ell_d}$ by

$$\mathcal{E}_{i, \ell_1, \ell_2, \dots, \ell_d} *_{d+1} f(\mathcal{A}) *_{d+1} \mathcal{E}, \quad (9)$$

where $\mathcal{E} \in \mathbb{R}^{N \times K_1 \times \dots \times K_d}$ is a tensor with all entries equal to one, and the *multilayer total communicability* by

$$\mathcal{E} *_{d+1} f(\mathcal{A}) *_{d+1} \mathcal{E}. \quad (10)$$

The latter definitions generalize analogous notions introduced for single-layer networks by Benzi and Klymko [5] and Katz [27] for f being the matrix exponential or a matrix resolvent. We refer to the quantity defined in (9) as the *multilayer Katz centrality* when f is the tensor resolvent.

For small networks, we can evaluate the tensor functions discussed above by applying the flattening operator mat , its inverse mat^{-1} , Proposition 1, and using the following result.

Proposition 4. *Let the tensor function f be defined by (3) with a power series that converges sufficiently rapidly. Then*

$$f(\mathcal{A}) = \text{mat}^{-1}(f(\text{mat}(\mathcal{A}))).$$

Proof: By Proposition 1, $\text{mat}(\mathcal{A}^p) = (\text{mat}(\mathcal{A}))^p$. Hence, $\sum_{p=1}^n \text{mat}(c_p \mathcal{A}^p) = \sum_{p=1}^n c_p (\text{mat}(\mathcal{A}))^p$ and we have

$$f(\text{mat}(\mathcal{A})) = \lim_{n \rightarrow \infty} \sum_{p=1}^n c_p (\text{mat}(\mathcal{A}))^p = \lim_{n \rightarrow \infty} \text{mat} \left(\sum_{p=1}^n c_p \mathcal{A}^p \right),$$

and by the definition of mat , we can write

$$\lim_{n \rightarrow \infty} \text{mat} \left(\sum_{p=1}^n c_p \mathcal{A}^p \right) = \text{mat} \left(\lim_{n \rightarrow \infty} \sum_{p=1}^n c_p \mathcal{A}^p \right).$$

Thus, one has

$$\text{mat}(f(\mathcal{A})) = f(\text{mat}(\mathcal{A})).$$

Applying the inverse operator mat^{-1} to both sides concludes the proof. \square

The evaluation of tensor functions using the above proposition is feasible for tensors that represent small to medium-sized multilayer networks. However, the computations are very demanding for large-scale multilayer networks. Approximations of tensor functions for the latter kind of networks can be computed

fairly inexpensively by applying Krylov subspace methods to the flattened adjacency tensor, i.e., supra-adjacency matrix, as in [7]. However, our main goal is to contribute to the development of a formalism where tensors are used. Therefore, we suggest computing communicability and centrality measures using Krylov subspace methods based on the tensor format. This is discussed in the following section.

4. Krylov subspace methods

Krylov subspace methods are well suited to approximate many matrix functions; see, e.g., [2, 23] for illustrations. They also have been applied successfully to the approximation of tensor functions and the solution of tensor systems of equations; see [3, 4, 15, 24, 31] and references therein. It is therefore natural to seek to approximate the tensor functions mentioned in the previous section by Krylov subspace methods. We first discuss the application of the global tensor Arnoldi process to the approximation of multilayer centrality measures, and subsequently consider the tensor block Arnoldi process.

4.1. A global tensor Arnoldi process based on the Einstein product

The global matrix Arnoldi process is a Krylov subspace method that was introduced by Jbilou et al. [25, 26] for the reduction of a large matrix to a small one. A global tensor Arnoldi process for the reduction of a large tensor to a small matrix using the Einstein product is described by El Guide et al. [15]. The application of m steps of the latter process to the tensor $\mathcal{A} \in \mathbb{R}^{N \times K_1 \times \dots \times K_d \times N \times K_1 \times \dots \times K_d}$ with initial tensor $\mathcal{V} \in \mathbb{R}^{N \times K_1 \times \dots \times K_d}$ determines, when no breakdown occurs, an orthonormal basis for the tensor Krylov subspace

$$\mathcal{K}_{m+1}(\mathcal{A}, \mathcal{V}) = \text{span}\{\mathcal{V}, \mathcal{A} *_{d+1} \mathcal{V}, \dots, \mathcal{A}^m *_{d+1} \mathcal{V}\} := \left\{ \sum_{i=0}^m \omega_i \mathcal{A}^i *_{d+1} \mathcal{V}, \omega_i \in \mathbb{R} \right\}. \quad (11)$$

This definition of the subspace is analogous to the definition of the solution subspace for global matrix methods used in [26].

The computations are described by Algorithm 1. The algorithm is said to *break down* at step j if $h_{i+1,i} > 0$ for $1 \leq i < j$ and $h_{j+1,j} = 0$. In the absence of breakdown, the algorithm determines the tensor $\mathbb{V}_{m+1} = [\mathcal{V}_1, \mathcal{V}_2, \dots, \mathcal{V}_{m+1}] \in \mathbb{R}^{N \times K_1 \times \dots \times K_d \times (m+1)}$ with orthonormal block columns, i.e.,

$$\langle \mathcal{V}_i, \mathcal{V}_j \rangle := \mathcal{V}_i *_{d+1} \mathcal{V}_j = \begin{cases} 1, & i = j, \\ 0, & i \neq j, \end{cases}$$

that span the tensor Krylov subspace $\mathcal{K}_{m+1}(\mathcal{A}, \mathcal{V})$. In line 5 of Algorithm 1, we have

$$\mathcal{A} *_{d+1} \mathbb{V}_j = [\mathcal{A} *_{d+1} \mathcal{V}_1, \mathcal{A} *_{d+1} \mathcal{V}_2, \dots, \mathcal{A} *_{d+1} \mathcal{V}_j] \in \mathbb{R}^{N \times K_1 \times \dots \times K_d \times j}.$$

Algorithm 1 Global tensor Arnoldi process

1: **Input:** Adjacency tensor $\mathcal{A} \in \mathbb{R}^{N \times K_1 \times \dots \times K_d \times N \times K_1 \times \dots \times K_d}$, initial tensor $\mathcal{V} \in \mathbb{R}^{N \times K_1 \times \dots \times K_d}$, and number of steps m .

2: **Output:** Orthonormal basis $\mathbb{V}_{m+1} = \{\mathcal{V}_1, \mathcal{V}_2, \dots, \mathcal{V}_{m+1}\}$ for the tensor Krylov subspace (11) and nontrivial entries of the upper Hessenberg matrix $H_{m+1,m} = [h_{ij}] \in \mathbb{R}^{(m+1) \times m}$.

3: $\mathcal{V}_1 = \mathcal{V} / \|\mathcal{V}\|_F$

4: **for** $j = 1, \dots, m$ **do**

5: $\mathcal{W} = \mathcal{A} *_{d+1} \mathcal{V}_j$

6: **for** $i = 1, \dots, j$ **do**

7: $h_{i,j} = \langle \mathcal{V}_i, \mathcal{W} \rangle$

8: $\mathcal{W} = \mathcal{W} - h_{i,j} \mathcal{V}_i$

9: **end for**

10: $h_{j+1,j} = \|\mathcal{W}\|_F$

11: **if** $h_{j+1,j} = 0$, **then stop**

12: **else** $\mathcal{V}_{j+1} = \mathcal{W} / h_{j+1,j}$

13: **end if**

14: **end for**

It follows from the recursion relation of Algorithm 1 that

$$\mathcal{A} *_{d+1} \mathbb{V}_m = \mathbb{V}_{m+1} *_{1} H_{m+1,m}, \quad (12)$$

where $H_{m+1,m} = [h_{ij}] \in \mathbb{R}^{(m+1) \times m}$ is an upper Hessenberg matrix made up of the coefficients h_{ij} generated in lines 7 and 10 of Algorithm 1; all entries below the subdiagonal of $H_{m+1,m}$ vanish.

Let the matrix $H_m \in \mathbb{R}^{m \times m}$ be obtained by deleting the last row of $H_{m+1,m}$. Then

$$\mathbb{V}_m^T *_{d+1} \mathcal{A} *_{d+1} \mathbb{V}_m = H_m,$$

where $\mathbb{V}_m = [\mathcal{V}_1, \mathcal{V}_2, \dots, \mathcal{V}_m] \in \mathbb{R}^{N \times K_1 \times \dots \times K_d \times m}$ and $\mathbb{V}_m^T = [\mathcal{V}_1, \mathcal{V}_2, \dots, \mathcal{V}_m]^T \in \mathbb{R}^{m \times N \times K_1 \times \dots \times K_d}$. Hence, H_m is the orthogonal projection of \mathcal{A} onto the subspace $\mathcal{K}_m(\mathcal{A}, \mathcal{V})$ with respect to the basis \mathbb{V}_m . This suggests to use the approximation

$$\mathbb{V}_m *_{1} f(H_m) *_{1} E_1 \|\mathcal{V}\|_F \quad (13)$$

of $f(\mathcal{A}) *_{d+1} \mathcal{V}$, where $\|\mathcal{V}\|_F = \sqrt{\mathbb{V}^T *_{d+1} \mathbb{V}}$ and $E_1 \in \mathbb{R}^m$ is the first vector from the canonical basis, analogously to the approach used when \mathcal{A} is a square matrix and \mathcal{V} is a vector; see [2, 15, 24].

This approach to approximate $f(\mathcal{A}) *_{d+1} \mathcal{V}$ works well when $\mathcal{V} = \mathcal{E}$ and can be applied to determine accurate approximations of the multilayer total communicability (10) and the multilayer total communicability of node $v_i^{\ell_1, \dots, \ell_d}$ defined by (9). The former is approximated by

$$\mathcal{E} *_{d+1} \mathbb{V}_m *_{1} f(H_m) *_{1} E_1 \|\mathcal{V}\|_F$$

and the latter by

$$\mathcal{E}_{i,\ell_1,\dots,\ell_d} *_{d+1} \mathbb{V}_m *_{1} f(H_m) *_{1} E_1 \|\mathcal{V}\|_F. \quad (14)$$

In particular, the evaluation of (14) does not require any arithmetic work when the expression (13) is available. This makes the evaluation of the multilayer total communicability of all nodes $v_i^{\ell_1,\dots,\ell_d}$, $1 \leq i \leq N$ and $1 \leq \ell_s \leq K_s$, $1 \leq s \leq d$, inexpensive when the expression (13) is known. We use this fact when determining nodes for which this measure is large in Section 5.

However, Algorithm 1 often suffers from breakdown when seeking to approximate an expression of the form $f(\mathcal{A}) *_{d+1} \mathcal{V}$ when the tensor \mathcal{V} is sparse, i.e., when \mathcal{V} has many vanishing entries. This is the case when seeking to approximate the subgraph centrality (5) by

$$\mathcal{E}_{i,\ell_1,\dots,\ell_d} *_{d+1} \mathbb{V}_m *_{1} f(H_m) *_{1} E_1 \|\mathcal{E}_{i,\ell_1,\dots,\ell_d}\|_F,$$

or the communicability (4) between the node $v_i^{\ell_1,\dots,\ell_d}$ and node $v_j^{k_1,\dots,k_d}$ by

$$\mathcal{E}_{i,\ell_1,\dots,\ell_d} *_{d+1} \mathbb{V}_m *_{1} f(H_m) *_{1} E_1 \|\mathcal{E}_{j,k_1,\dots,k_d}\|_F.$$

When computing these approximations, the initial block tensor is $\mathcal{V} = \mathcal{E}_{i,\ell_1,\dots,\ell_d}$, which is very sparse. Since the tensor \mathcal{A} typically also is sparse, this often results in that the scalar $h_{j+1,j}$ in line 10 of Algorithm 1 vanishes for some $1 \leq j \leq m$. The computations with the algorithm then cannot be continued, and the available expression at breakdown,

$$\mathbb{V}_j *_{1} f(H_j) *_{1} E_1 \|\mathcal{V}\|_F,$$

might not furnish an approximation of desired accuracy. Moreover, even when all the multilayer subgraph centralities can be computed to determine the node with the largest subgraph centrality, this is quite expensive for large multilayer networks. We describe in the following subsection how these difficulties can be reduced by replacing the initial tensor \mathcal{V} in Algorithm 1 by a block of tensors.

4.2. A block Arnoldi process based on the Einstein product

We describe a block Arnoldi process that uses the Einstein product. It differs from Algorithm 1 in that the initial tensor \mathcal{V} is extended to a block tensor. The application of m steps of the block Arnoldi process to \mathcal{A} with initial tensor \mathcal{W} determines, in the absence of breakdown, an orthonormal basis for the block tensor Krylov subspace

$$\begin{aligned} \mathcal{K}_{m+1}^{\text{block}}(\mathcal{A}, \mathcal{W}) &= \text{range}\{\mathcal{W}, \mathcal{A} *_{d+1} \mathcal{W}, \dots, \mathcal{A}^m *_{d+1} \mathcal{W}\} \\ &= \left\{ \sum_{i=0}^m \mathcal{A}^i *_{d+1} \mathcal{W} *_{1} \Omega_i, \Omega_i \in \mathbb{R}^{P \times P} \right\}, \end{aligned} \quad (15)$$

where $\mathcal{W} \in \mathbb{R}^{N \times K_1 \times \dots \times K_d \times P}$. We will refer to the integer P as the block size. This definition of the subspace is analogous to the definition of the solution

subspace for block matrix methods used in [26]. The block Arnoldi process of this subsection has the advantage of typically requiring fewer accesses to the adjacency tensor than when applying Algorithm 1. Moreover, choosing suitable auxiliary columns in the initial tensor \mathcal{W} , the occurrences of breakdowns can be reduced in comparison with Algorithm 1. The block Arnoldi process is summarized by Algorithm 2.

Algorithm 2 Block tensor Arnoldi process

- 1: **Input:** Adjacency tensor $A \in \mathbb{R}^{N \times K_1 \times \dots \times K_d \times N \times K_1 \times \dots \times K_d}$, initial tensor $\mathcal{W} \in \mathbb{R}^{N \times K_1 \times \dots \times K_d \times P}$, and number of steps m .
 - 2: **Output:** Orthonormal basis $\mathbb{W}_{m+1} = \{\mathcal{W}_1, \mathcal{W}_2, \dots, \mathcal{W}_{m+1}\}$ for the block Krylov subspace (15), and nontrivial entries $H_{i,j} \in \mathbb{R}^{P \times P}$ of the upper block Hessenberg matrix $\mathbb{H}_{m+1,m} = [H_{i,j}] \in \mathbb{R}^{P(m+1) \times Pm}$.
 - 3: Compute the QR factorization $\mathcal{W} = \mathcal{Q} *_1 R$, where the tensor $\mathcal{Q} \in \mathbb{R}^{N \times K_1 \times \dots \times K_d \times P}$ satisfies $\mathcal{Q}^T *_1 \mathcal{Q} = \mathcal{I}$ and the matrix $R \in \mathbb{R}^{P \times P}$ is upper triangular. Set $\mathcal{W}_1 = \mathcal{Q}$ and $H_{1,0} = R$.
 - 4: **for** $j = 1, \dots, m$ **do**
 - 5: $\mathcal{U} = \mathcal{A} *_d \mathcal{W}_j$
 - 6: **for** $i = 1, \dots, j$ **do**
 - 7: $H_{i,j} = \mathcal{W}_i^T *_d \mathcal{U}$,
 - 8: $\mathcal{U} = \mathcal{U} - \mathcal{W}_i *_1 H_{i,j}$
 - 9: **end for**
 - 10: Compute the QR factorization $\mathcal{U} = \mathcal{Q} *_1 R$, where $\mathcal{Q} \in \mathbb{R}^{N \times K_1 \times \dots \times K_d \times P}$ satisfies $\mathcal{Q}^T *_1 \mathcal{Q} = \mathcal{I}$ and the matrix $R \in \mathbb{R}^{P \times P}$ is upper triangular. Set $\mathcal{W}_{j+1} = \mathcal{Q}$ and $H_{j+1,j} = R$.
 - 11: **end for**
-

Algorithm 2 determines an orthonormal basis

$$\mathbb{W}_{m+1} = [\mathcal{W}_1, \dots, \mathcal{W}_{m+1}] \in \mathbb{R}^{N \times K_1 \times \dots \times K_d \times P(m+1)}$$

for the block Krylov subspace (15) and the upper block Hessenberg matrix

$$\mathbb{H}_{m+1,m} = \begin{bmatrix} H_{1,1} & H_{1,2} & H_{1,3} & \cdots & H_{1,m-1} & H_{1,m} \\ H_{2,1} & H_{2,2} & H_{2,3} & \cdots & H_{2,m-1} & H_{2,m} \\ & H_{3,2} & H_{3,3} & \cdots & H_{3,m-1} & H_{3,m} \\ & & \ddots & & \vdots & \vdots \\ & & & & H_{m,m-1} & H_{m,m} \\ & & & & & H_{m+1,m} \end{bmatrix} \in \mathbb{R}^{P(m+1) \times Pm}.$$

Its leading $Pm \times Pm$ submatrix is denoted by \mathbb{H}_m . We have the following result:

Proposition 5. *Suppose that m steps of Algorithm 2 have been carried out. Then*

$$\mathcal{A} *_d \mathbb{W}_m = \mathbb{W}_{m+1} *_1 \mathbb{H}_{m+1,m} \quad (16)$$

and

$$\mathcal{A} *_{d+1} \mathbb{W}_m = \mathbb{W}_m *_{\mathbb{H}_m} + \mathcal{W}_{m+1} *_{H_{m+1,m}} *_{\mathbb{E}_m^T}, \quad (17)$$

where $\mathbb{W}_m = [\mathcal{W}_1, \dots, \mathcal{W}_m] \in \mathbb{R}^{N \times K_1 \times \dots \times K_d \times Pm}$ is made up of the first m tensor columns of \mathbb{W}_{m+1} and $\mathbb{E}_m^T = [0, 0, \dots, I_P] \in \mathbb{R}^{P \times Pm}$. Moreover,

$$\mathcal{A}^p *_{d+1} \mathcal{W} = \mathbb{W}_m *_{\mathbb{H}_m^p} *_{E_1 \chi_0}, \quad (18)$$

where χ_0 is obtained from the QR factorization of \mathcal{W} , such that $\mathcal{W} = \mathbb{W}_m *_{E_1 \chi_0}$ holds for all $p \leq 0$.

Proof: For $1 \leq j \leq m$, one has

$$\begin{aligned} & [\mathbb{W}_{m+1} *_{\mathbb{H}_{m+1,m}}]_{:, \dots, :, 1+P(j-1):Pj} \\ &= \sum_{i=1}^{j+1} (\mathbb{W}_{m+1})_{:, \dots, :, 1+P(i-1):Pi} *_{(\mathbb{H}_{m+1,m})_{1+P(i-1):Pi, 1+P(j-1):Pj}} \\ &= [\mathcal{A} *_{d+1} \mathbb{W}_m]_{:, \dots, :, 1+P(j-1):Pj}. \end{aligned}$$

This leads to equation (16); equation (17) can be shown similarly. The last claim can be proved by induction. In fact, if $p = 0$, then one has $\mathcal{A}^0 *_{d+1} \mathcal{W} = \mathcal{W} = \mathbb{W}_m *_{E_1 \chi_0}$ and, by assuming that (18) holds for $p \geq 0$, one obtains

$$\mathcal{A}^{p+1} *_{d+1} \mathcal{W} = \mathcal{A} *_{d+1} \mathcal{A}^p *_{d+1} \mathcal{W} = \mathcal{A} *_{d+1} \mathbb{W}_m *_{\mathbb{H}_m^p} *_{E_1 \chi_0},$$

so that, using equation (17), we have

$$\begin{aligned} \mathcal{A}^{p+1} *_{d+1} \mathcal{W} &= (\mathbb{W}_m *_{\mathbb{H}_m} + \mathcal{W}_{m+1} *_{H_{m+1,m}} *_{\mathbb{E}_m^T}) *_{\mathbb{H}_m^p} *_{E_1 \chi_0} \\ &= \mathbb{W}_m *_{\mathbb{H}_m} *_{\mathbb{H}_m^p} *_{E_1 \chi_0} \\ &\quad + \mathcal{W}_{m+1} *_{H_{m+1,m}} *_{\mathbb{E}_m^T} *_{\mathbb{H}_m^p} *_{E_1 \chi_0}, \end{aligned}$$

where the second term vanishes due to the fact that \mathbb{H}_m is a block Hessenberg matrix. This concludes the proof. \square

Thanks to equation (18), $f(\mathcal{A}) *_{d+1} \mathcal{W}$ can be approximated by

$$\mathbb{W}_m *_{d+1} f(\mathbb{H}_m) *_{E_1 \chi_0}, \quad (19)$$

where χ_0 is such that $\mathcal{W} = \mathbb{W}_m *_{E_1 \chi_0}$. The advantage of this approach is that we can compute the multilayer subgraph centrality and the resolvent-based subgraph centrality of P nodes at once, and we also can determine approximations of the multilayer communicabilities of these P nodes essentially for free. This is because we are approximating the quantity $f(\mathcal{A}) *_{d+1} \mathcal{W}$ by (19), and then can evaluate the approximation $\mathcal{W}^T *_{d+1} \mathbb{W}_m *_{d+1} f(\mathbb{H}_m) *_{E_1 \chi_0}$ of $\mathcal{W}^T *_{d+1} f(\mathcal{A}) *_{d+1} \mathcal{W}$ inexpensively. Moreover, we can circumvent the numerical stability issue related to the sparsity of the adjacency tensor and the initial block by adding a dense tensor in the initial block tensor. This technique has been discussed for matrix functions case in [22]. Notice that if we include \mathcal{E} , i.e., the tensor of all ones, in the initial block tensor, then Algorithm 2 will produce

the same quantities of interest as one would compute with Algorithm 1 when applied with the initial tensor $\mathcal{V} = \mathcal{E}$, as well as the multilayer total network communicability. This is because once we approximate

$$f(\mathcal{A}) *_{d+1} \mathcal{W} := [f(\mathcal{A}) *_{d+1} \mathcal{W}_1, \dots, f(\mathcal{A}) *_{d+1} \mathcal{W}_P, f(\mathcal{A}) *_{d+1} \mathcal{W}_{P+1}],$$

where $\mathcal{W}_{P+1} = \mathcal{E}$, we only need to compute the following Einstein product $M := \mathcal{W}^T *_{d+1} f(\mathcal{A}) *_{d+1} \mathcal{W} \in \mathbb{R}^{P+1 \times P+1}$. Then for $1 \leq i, j \leq P$ and $i \neq j$ the quantities $M_{i,j}$ are the communicabilities between different nodes, for $1 \leq i \leq P$ the quantities $M_{i,i}$ are the multilayer subgraph centralities, for $1 \leq i \leq P$ the quantities $M_{i,P+1}$ are the same obtained by Algorithm 1, and $M_{P+1,P+1}$ is the multilayer total network communicability of the whole network.

5. Computed examples

This section presents some examples to illustrate the performance of the methods discussed above. The computations were carried out using MATLAB R2015b. We use the Matlab library, tensor toolbox [28], to perform operations on tensors. For the examples in Sections 5.2 and 5.3, we choose the minimum number of steps, m , with the Krylov subspace method needed to obtain the same ranking of the first 10 nodes as the ranking obtained when evaluating the exact tensor function. We will see that the number of steps required is quite small. Due to the size of the networks in the examples in Sections 5.4 and 5.5, it is expensive to evaluate the exact tensor function. In these examples, we therefore increase the number of steps, m , of the Krylov subspace until the ranking does not change, and consider the ranking so obtained the exact one. Knowledge of the nodes for which we are interest in computing multilayer subgraph centrality is needed for Algorithm 2. We choose these nodes as the top central ones obtained by Algorithm 1.

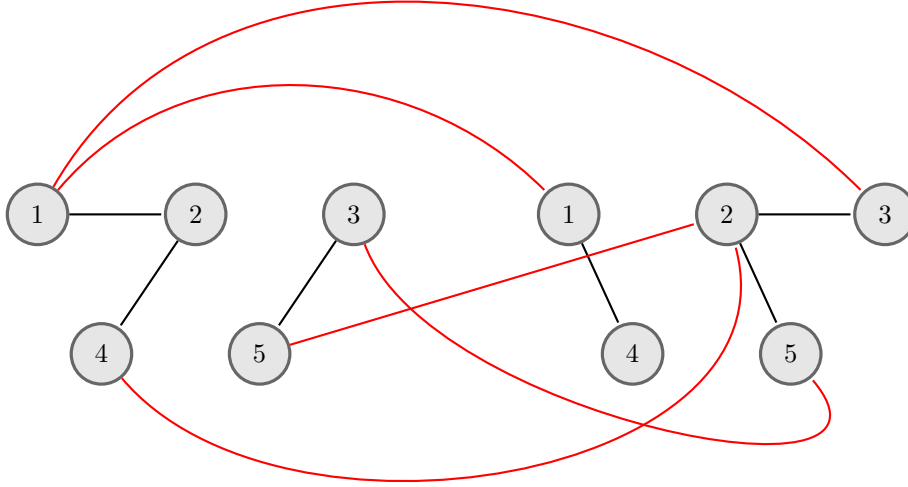


Figure 2: Example 1: Layers are presented from left to right in the order $L = 1$ and $L = 2$. The edges connecting nodes from same layer are marked in black. The edges connecting nodes from different layers are marked in red.

5.1. Example 1: A small synthetic multilayer network

Consider a small synthetic unweighted and undirected multilayer network with $d = 1$, $K_1 = 2$, and $N = 5$. It consists of 10 edges as shown by the graph of Figure 2. Let \mathcal{A} be the adjacency tensor. We compute the different multilayer centrality measures discussed using the Einstein product. The results are summarized in Table 1 for $\beta = 1$ and $\alpha = 0.5/\lambda_{max}$. We can see that node v_2^2 has the largest centrality measures and, therefore, is the most important node. This node is followed by node v_1^1 . Node v_4^2 is the least important node. All centrality measures perform as can be expected.

5.2. Example 2: A synthetic multilayer network

We consider an example of a weighted multilayer network with $d = 1$ aspect, $K_1 = 32$ layers, $N = 20$ nodes, and 674 edges. The network can be downloaded from <https://github.com/wjj0301/Multiplex-Networks>. We compute approximations of the multilayer total communicability of the nodes v_i^ℓ and multilayer Katz centrality using Algorithm 1, as well as the exact multilayer total communicability of the nodes v_i^ℓ and multilayer Katz centrality, i.e., the subgraph centrality determined with the function (8), by flattening the adjacency tensor and using the MATLAB function `expm` and the MATLAB backslash operator when using the function (8). The errors in the computed approximations

Table 1: Multilayer total communicability of the nodes v_i^ℓ (MTC), multilayer Katz centrality (MKC), multilayer subgraph centrality with the modified tensor exponential (MSC_{exp_0}), multilayer subgraph centrality with the modified tensor resolvent (MSC_{res_0}) for the nodes of Example 1.

v_i^ℓ	$MTC(i, \ell)$		$MKC(i, \ell)$	
	$\ell = 1$	$\ell = 2$	$\ell = 1$	$\ell = 2$
$i = 1$	12.2520	7.7379	2.1131	1.7044
$i = 2$	9.6537	17.2450	1.8145	2.5454
$i = 3$	8.9474	11.7351	1.7645	1.9484
$i = 4$	10.8250	4.2550	1.8876	1.3470
$i = 5$	10.6175	10.6175	1.8774	1.8774
v_i^ℓ	$MSC_{\text{exp}_0}(i, \ell)$		$MSC_{\text{res}_0}(i, \ell)$	
	$\ell = 1$	$\ell = 2$	$\ell = 1$	$\ell = 2$
$i = 1$	3.1001	2.2834	1.1507	1.0952
$i = 2$	2.3582	4.1313	1.0987	1.2165
$i = 3$	2.3946	2.4698	1.1003	1.1039
$i = 4$	2.4174	1.5922	1.1016	1.0454
$i = 5$	2.5001	2.5001	1.1051	1.1051

are determined by the vector infinity norm, that is, the exact multilayer total communicability of the nodes, multilayer Katz centrality, and their approximations are stored in vectors and the infinity norm is applied to measure the distance between the vectors with the exact entries and the vectors with the corresponding entries determined by Krylov subspace methods. Figure 3 displays the errors as a function of the Krylov subspace dimension m . Table 2 lists the top 10 central nodes according to the multilayer total communicability with respect to a node and multilayer Katz centrality. We notice that the multilayer Katz centrality is approximated accurately when the same number of steps, m , of Algorithm 1 are carried out. The multilayer total communicability of the nodes is approximated less accurately with the same number of steps, but still gives the same ranking of nodes as when the exact communicability is used.

We also set the weight of all edges to one to obtain an unweighted multilayer network and compute the multilayer total communicability of the nodes and multilayer Katz centrality. We notice that the multilayer total communicability of the nodes is approximated accurately when $m = 6$ steps of Algorithm 1 are carried out also for larger values of β . However, the multilayer Katz centrality is not approximated accurately for $m = 6$ steps when $\alpha > 0.66/\lambda_{\max}$. Figure 3 depicts the influence of the values of α and β on the dimension of Krylov subspace needed to obtain accurate approximations for both weighted and unweighted graphs.

Finally, we turn to the computation of multilayer subgraph centralities of some nodes. We apply Algorithm 2 to our adjacency tensor with the first block $\mathcal{V} \in \mathbb{R}^{N \times K_1 \times P}$ with P frontal slices of the form $E_{i,\ell}$. We let $P = 10$ and choose the indices $\{i, \ell\}$ randomly. The results obtained are summarized in Table 3, which also shows communicabilities that we obtain for free since we use a block

Table 2: Top 10 central nodes determined by Algorithm 1 with $m = 6$ using the (approximate) multilayer total communicability of the nodes (MTC) and (approximate) multilayer Katz centrality (MKC) so obtained for the weighted multilayer network in Example 2, with $\alpha = 0.4/\lambda_{\max}$ and $\beta = 0.4$. These computed values are compared to the exact ones obtained by flattening and using matrix functions.

$\{i, \ell\}$	$MTC\{i, \ell\}$	$MTC_{\text{exact}}\{i, \ell\}$	$\{i, \ell\}$	$MKC\{i, \ell\}$	$MKC_{\text{exact}}\{i, \ell\}$
{18, 24}	99.4969	97.1435	{18, 24}	3.6474	3.6407
{17, 26}	70.0610	72.6593	{19, 19}	3.0148	3.0191
{13, 19}	64.5009	67.7357	{14, 23}	2.8966	2.8956
{8, 26}	62.8084	67.1222	{13, 19}	2.6318	2.6407
{19, 19}	62.1558	63.7426	{17, 26}	2.6242	2.6313
{6, 24}	59.3319	60.2469	{6, 29}	2.5999	2.5990
{19, 4}	58.9334	59.4300	{2, 29}	2.5497	2.5477
{14, 24}	56.5841	56.4157	{1, 32}	2.5371	2.5425
{1, 32}	52.8265	54.7537	{1, 3}	2.5251	2.5240
{2, 24}	51.6585	54.3109	{14, 24}	2.5150	2.5146

Table 3: Multilayer subgraph centrality obtained with the modified tensor exponential (MSC_{exp_0}) and multilayer subgraph centrality with the modified tensor resolvent (MSC_{reso}) for some nodes for the unweighted multilayer network in Example 2, as well as free multilayer communicabilities of the nodes (MC) with $\alpha = 0.5/\lambda_{\max}$, $\beta = 1$, and $m = 5$.

$\{i, \ell\}$	$MSC_{\text{exp}_0}\{i, \ell\}$	$MSC_{\text{reso}}\{i, \ell\}$	$\{i, \ell, j, k\}$	$MC\{i, \ell, j, k\}$
{4, 1}	1.1683	1.0358		
{5, 1}	1.2116	1.0488		
{12, 1}	1.5878	1.1321		
{1, 3}	1.1766	1.0395	{5, 1, 4, 1}	1.0505
{19, 4}	1.0084	1.0038	{12, 1, 4, 1}	0.1768
{2, 11}	1.0592	1.0193	{12, 1, 5, 1}	0.5531
{13, 18}	1.1681	1.0354	{13, 18, 19, 18}	0.0502
{19, 18}	1.0097	1.0048		
{14, 22}	1.2537	1.0611		
{8, 25}	1.5431	1.1176		

method.

5.3. Example 3: Multiplex network (Scotland Yard transportation data)

This example considers the Scotland Yard transportation network created by the authors of [7], which is a multiplex network. A multiplex network is a special case of a multilayer network. The network can be downloaded from [6] as a weighted or unweighted multiplex network. It consists of 3324 edges and $N = 199$ nodes that represent public transport stops in the city of London. The network has $K_1 = 4$ layers that represent different modes of transportation: Boat, underground, bus, and taxi. The weights are determined so that the edges in the layer that represent travel by taxi all have weight one. A taxi ride is defined as a trip by taxi between two adjacent nodes in the taxi layer; a taxi ride along k edges is considered k taxi rides. The weights of edges in the boat,

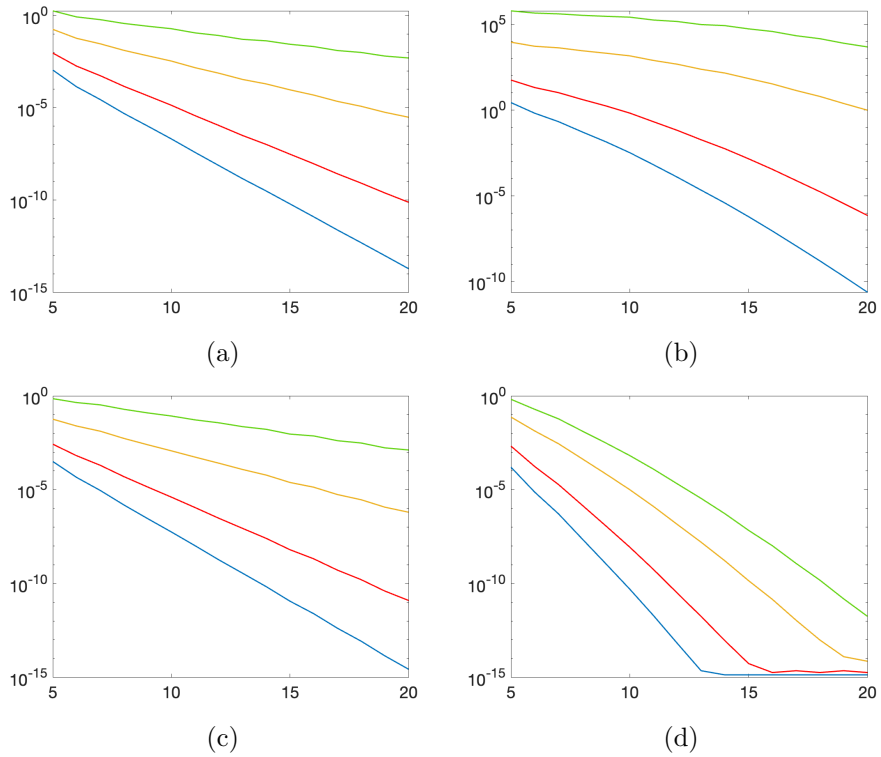


Figure 3: Infinity norm error for multilayer total communicability of the nodes and multilayer Katz centrality as functions of the Krylov subspace dimension m for Example 2 with $\alpha \in \left\{ \frac{0.2}{\lambda_{\max}}, \frac{0.3}{\lambda_{\max}}, \frac{0.5}{\lambda_{\max}}, \frac{0.7}{\lambda_{\max}} \right\}$, and $\beta \in \{0.3, 0.5, 1, 1.5\}$ ({blue, red, yellow, green}). (a) multilayer Katz centrality for weighted edges, (b) multilayer total communicability of the nodes for weighted edges, (c) multilayer Katz centrality for unweighted edges, and (d) multilayer total communicability of the nodes for unweighted edges.

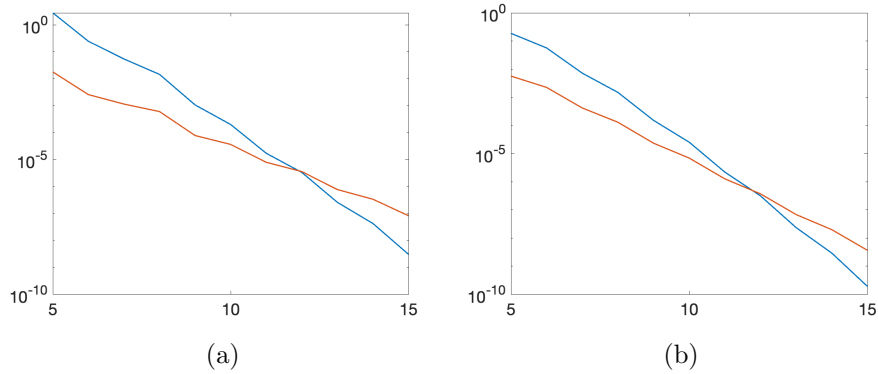


Figure 4: Infinity norm error for multilayer total communicability of the nodes (blue) and multilayer Katz centrality (orange) as functions of the Krylov subspace dimension m for Example 3. (a) when edges are unweighted and $\alpha = 0.4/\lambda_{\max}$ and $\beta = 0.4$, (b) when edges are weighted and $\alpha = 0.3/\lambda_{\max}$ and $\beta = 0.1$.

Table 4: Multilayer subgraph centrality obtained with the modified tensor exponential (MSC_{exp_0}) and multilayer subgraph centrality with the modified tensor resolvent (MSC_{res_0}) for some nodes of the network in Example 3, with $\alpha = 0.3/\lambda_{\max}$, $\beta = 0.3$, $P = 11$ and $m = 10$.

$\{i, \ell\}$	$MSC_{\text{exp}_0}\{i, \ell\}$	$MSC_{\text{res}_0}\{i, \ell\}$
{142,4}	1.6080	1.0345
{140,4}	1.5004	1.0295
{58,4}	1.5182	1.0301
{128,4}	1.4583	1.0267
{67,3}	1.4442	1.0262
{153,4}	1.4457	1.0263
{143,4}	1.4754	1.0273
{114,4}	1.4933	1.0293
{129,4}	1.4647	1.0269
{128,3}	1.4519	1.0265

underground, and bus layers are chosen to be equal to the minimal number of taxi rides required to travel between the same nodes. We compute the multilayer Katz centrality and multilayer total communicability of the nodes by applying Algorithm 1 to the adjacency tensor of the given multiplex network, as well as to the adjacency tensor of the associated unweighted network; in the latter adjacency tensor all edges have weight one. We compute the exact multilayer Katz centrality and multilayer total communicability of the nodes in the same way as in the previous example and evaluate the infinity norm error as well. Figure 4 displays the errors as a function of the Krylov subspace dimension. This illustrates the accuracy of Algorithm 1 when applied to multiplex networks.

We also compute the multilayer subgraph centrality (MSC) measures for the top 10 nodes using Algorithm 2; see Table 4. The total network communicability obtained is $3.904 \cdot 10^3$. Multilayer communicabilities between some of the nodes considered are listed in Table 5.

Table 5: Multilayer communicabilities obtained with the modified tensor exponential (MC_{exp_0}) and with the modified tensor resolvent (MC_{res_0}) for some nodes of the network in Example 3, with $\alpha = 0.3/\lambda_{\max}$, $\beta = 0.3$, $P = 11$ and $m = 10$.

$\{i, \ell, j, k\}$	MC_{exp_0}	MC_{res_0}
$\{128, 4, 142, 4\}$	0.4666	0.0614
$\{153, 4, 140, 4\}$	0.1267	0.0070
$\{142, 4, 143, 4\}$	0.5192	0.0646
$\{128, 3, 128, 4\}$	0.5010	0.0640
$\{67, 3, 153, 4\}$	$7.0328 \cdot 10^{-4}$	$1.8124 \cdot 10^{-4}$

5.4. Example 4: Multiplex network (European airlines data set)

The European airlines data set consists of $N = 450$ nodes that represent European airports and has $K_1 = 37$ layers that represent different airlines operating in Europe. There are 3588 edges, which represent available routes. This network can be represented by a fourth-order adjacency tensor $\mathcal{A} \in \mathbb{R}^{N \times K_1 \times N \times K_1}$ such that $\mathcal{A}(i, \ell, j, \ell) = 1$ if there is a flight connecting airports i and j with airline ℓ . Moreover, $\mathcal{A}(i, \ell, i, k) = 1$ for every $1 \leq \ell, k \leq K_1$ to reflect the effort required to change airlines for connecting flights. The network can be downloaded from [6]. Similarly as Taylor et al. [34], we only include $N = 417$ nodes from the largest connected component of the network. We compute the multilayer total communicability of the nodes and the multilayer Katz centrality using Algorithm 1 to approximate the tensor exponential and the tensor resolvent functions. Table 6 lists the top 10 central nodes. We obtained similar ranking as reported in [7], where the authors applied Krylov subspace methods to the supra-adjacency matrix of the network in order to compute matrix function-based centrality measures such as the Katz centrality.

We apply Algorithm 2 to our adjacency tensor in order to compute the multilayer subgraph centrality (MSC) for the top 10 nodes determined earlier. This algorithm determines the multilayer subgraph centrality for the different nodes at once, the results are reported in Table 7. Table 8 shows the multilayer communicabilities between the considered nodes determined by the algorithm. The multilayer total network communicability is $2.4163 \cdot 10^7$.

5.5. Example 5: Wikispeedia network

This data set contains human navigation paths in Wikipedia, collected through the human-computation game Wikispeedia. Wikispeedia users are asked to navigate from a given source to a given target article, being allowed to click on links only. Nodes are articles of the English Wikipedia and edges represent clicks. The data is provided by the Stanford Network Analysis Project <http://snap.stanford.edu/index.html>. It contains 4604 articles and 119882 links. We classified the articles into 16 different subjects (Countries, Science, Geography, ...) and then built a multilayer network with $N = 4604$ nodes and $K_1 = 16$ layers. Each layer contains the edges connecting the nodes that are considered to be classified in this layer. We have used the files that contain node identifiers and all edges from <https://github.com/franloza/Wikispeedia-Network>.

Table 6: Top 10 central nodes according to multilayer total communicability of the nodes (MTC) and multilayer Katz centrality (MKC) for the European airlines network in Example 4, with $\alpha = 0.5/\lambda_{\max}$ and $\beta = 0.2$. The MTC and MKC values are computed with Algorithm 1 with $m = 20$.

$\{i, \ell\}$	$MTC\{i, \ell\}$	$\{i, \ell\}$	$MKC\{i, \ell\}$
{Stansted, Ryanair}	$8.2164 \cdot 10^3$	{Stansted, Ryanair}	4.4228
{Munich, Lufthansa}	$7.5209 \cdot 10^3$	{Munich, Lufthansa}	4.0937
{Frankfurt, Lufthansa}	$7.4541 \cdot 10^3$	{Frankfurt, Lufthansa}	4.0650
{Dublin, Ryanair}	$6.8942 \cdot 10^3$	{Ataturk, Turkish}	4.0486
{Gatwick, EasyJet}	$6.5714 \cdot 10^3$	{Gatwick, EasyJet}	3.7925
{Ataturk, Turkish}	$6.4399 \cdot 10^3$	{Dublin, Ryanair}	3.6479
{Amsterdam, KLM}	$6.0994 \cdot 10^3$	{Vienna, Austrian}	3.5939
{Vienna, Austrian}	$5.8057 \cdot 10^3$	{Amsterdam, KLM}	3.5661
{Caravaggio, Ryanair}	$5.7104 \cdot 10^3$	{Caravaggio, Ryanair}	3.3244
{Adolfo, Ryanair}	$5.5765 \cdot 10^3$	{Charles de Gaulle, Air France}	3.2444

Table 7: Multilayer subgraph centrality obtained with the modified tensor exponential (MSC_{exp_0}) and multilayer subgraph centrality with the modified tensor resolvent (MSC_{res_0}) for some nodes of the European airlines network in Example 4, with $\alpha = 0.5/\lambda_{\max}$, $\beta = 0.2$, $P = 11$, and $m = 10$.

$\{i, \ell\}$	$MSC_{\text{exp}_0}\{i, \ell\}$	$MSC_{\text{res}_0}\{i, \ell\}$
{Stansted, Ryanair}	53.6833	1.0282
{Munich, Lufthansa}	49.9200	1.0261
{Frankfurt, Lufthansa}	49.7844	1.0259
{Dublin, Ryanair}	49.0779	1.0225
{Gatwick, EasyJet}	47.2554	1.0239
{Ataturk, Turkish}	47.4633	1.0261
{Amsterdam, KLM}	45.1513	1.0224
{Vienna, Austrian}	45.2302	1.0228
{Caravaggio, Ryanair}	46.4080	1.0203
{Adolfo, Ryanair}	43.4764	1.0171

Table 8: Multilayer communicabilities obtained with the modified tensor exponential (MC_{exp_0}) and with the modified tensor resolvent (MC_{res_0}) for some nodes of the European airlines network in Example 4, with $\alpha = 0.5/\lambda_{\max}$, $\beta = 0.2$, $P = 11$, and $m = 10$.

$\{i, \ell, j, k\}$	MC_{exp_0}	MC_{res_0}
{Dublin, Ryanair, Stansted, Ryanair}	$1.33 \cdot 10^1$	$2.17 \cdot 10^{-2}$
{Vienna, Austrian, Stansted, Ryanair}	$6.56 \cdot 10^{-1}$	$4.37 \cdot 10^{-5}$
{Frankfurt, Lufthansa, Munich, Lufthansa}	$1.31 \cdot 10^1$	$2.46 \cdot 10^{-1}$
{Amsterdam, KLM, Frankfurt, Lufthansa}	$5.58 \cdot 10^0$	$8.96 \cdot 10^{-4}$
{Caravaggio, Ryanair, Dublin, Ryanair}	$1.01 \cdot 10^1$	$1.87 \cdot 10^{-2}$
{Stansted, Ryanair, Ataturk, Turkish}	$7.42 \cdot 10^{-1}$	$4.88 \cdot 10^{-5}$
{Munich, Lufthansa, Gatwick, EasyJet}	$3.53 \cdot 10^0$	$2.24 \cdot 10^{-4}$
{Caravaggio, Ryanair, Adolfo, Ryanair}	$7.94 \cdot 10^0$	$1.72 \cdot 10^{-2}$
{Ataturk, Turkish, Caravaggio, Ryanair}	$5.06 \cdot 10^{-1}$	$3.20 \cdot 10^{-5}$
{Stansted, Ryanair, Adolfo, Ryanair}	$9.41 \cdot 10^0$	$1.82 \cdot 10^{-2}$

Table 9: Top 10 central nodes according to the multilayer total communicability (MTC) and the multilayer Katz centrality (MKC) for the Wikispeedia network in Example 5, with $\beta = 0.2$, $\alpha = 0.5/\lambda_{\max}$. The MTC and MKC values are approximations determined by Algorithm 1 with $m = 20$.

$\{i, \ell\}$	$MTC\{i, \ell\}$
{Fauna of Australia, Science}	$2.3711 \cdot 10^{27}$
{Africa, Countries}	$2.1895 \cdot 10^{27}$
{Periodic table, Science}	$1.7854 \cdot 10^{27}$
{List of elements by name, Science}	$1.7241 \cdot 10^{27}$
{Periodic table (large version), Science}	$1.7162 \cdot 10^{27}$
{Bird, Science}	$1.5887 \cdot 10^{27}$
{Bird, Animals}	$1.5887 \cdot 10^{27}$
{President of the United States, Politics}	$1.5476 \cdot 10^{27}$
{Star, Science}	$1.5465 \cdot 10^{27}$
{Star, Space}	$1.5465 \cdot 10^{27}$
$\{i, \ell\}$	$MKC\{i, \ell\}$
{Lebanon, Geography}	4.7019
{Armenia, Countries}	4.5967
{Armenia, Geography}	4.5967
{Georgia, Countries}	4.5712
{Georgia, Geography}	4.5712
{Turkey, Countries}	4.4296
{Turkey, Geography}	4.4296
{Djibouti, Countries}	4.2680
{Djibouti, Geography}	4.2680
{Mozambique, Countries}	4.1781

We compute the multilayer Katz centrality and multilayer total communicability of the nodes by applying Algorithm 1 to the adjacency tensor of the given multilayer network. Table 9 lists the top 10 central nodes for this network.

5.6. Example 6: Synthetic multilayer network with 2 aspects

In this last example, we consider a weighted undirected multilayer network with $d = 2$ aspects, $K_1 = 3$, $K_2 = 2$ and $N = 180$ nodes. The data can be download from <https://github.com/wjj0301/Multiplex-Networks>, in the form of 6 layers then, transformed to a multilayer network with 2 aspects, it contains 148 edges in total. We compute the multilayer Katz centrality and multilayer total communicability of the nodes by applying Algorithm 1 to the 6^{th} order adjacency tensor $\mathcal{A} \in \mathbb{R}^{180 \times 3 \times 2 \times 180 \times 3 \times 2}$. Table 10 displays the top 10 central nodes. We apply Algorithm 2 to approximate the multilayer subgraph centrality measures for the top 10 central nodes determined by Algorithm 1 and the total network communicability which is $1.6088 \cdot 10^3$. Table 11 displays multilayer subgraph centrality measures obtained by Algorithm 2.

Table 10: Top 10 central nodes according to multilayer total communicability of the nodes (MTC) and multilayer Katz centrality (MKC) for the network in Example 6, with $\alpha = 0.5/\lambda_{\max}$ and $\beta = 0.2$. The MTC and MKC values are computed with Algorithm 1 with $m = 10$.

$\{i, \ell_1, \ell_2\}$	$MTC\{i, \ell_1, \ell_2\}$	$\{i, \ell_1, \ell_2\}$	$MKC\{i, \ell_1, \ell_2\}$
{2,4,1}	21.9603	{100,1,2}	1.0495
{26, 1, 1}	18.7547	{55,2,1}	0.9638
{100,1,2}	18.3988	{24,1,1}	0.9383
{115,1,2}	16.9789	{26,1,1}	0.8261
{27,1,1}	16.3683	{98,1,2}	0.8062
{6,1,1}	15.1006	{131,2,2}	0.7439
{99,1,2}	13.8501	{48,2,1}	0.7243
{172,3,2}	12.7657	{176,3,2}	0.6906
{176,3,2}	12.7579	{162,3,2}	0.6773
{13,1,1}	12.6350	{155,3,2}	0.6752

Table 11: Multilayer subgraph centrality obtained with the modified tensor exponential (MSC_{exp_0}) and multilayer subgraph centrality with the modified tensor resolvent (MSC_{res_0}) for some nodes of the network in Example 6, with $\alpha = 0.3/\lambda_{\max}$, $\beta = 0.3$, $P = 11$, and $m = 5$.

$\{i, \ell_1, \ell_2\}$	$MSC_{\text{exp}_0}\{i, \ell_1, \ell_2\}$	$MSC_{\text{res}_0}\{i, \ell_1, \ell_2\}$
{2,4,1}	2.5074	1.0082
{26, 1, 1}	2.5074	1.0082
{100,1,2}	1.0000	1.0000
{115,1,2}	1.0000	1.0000
{27,1,1}	2.5074	1.0082
{6,1,1}	2.5074	1.0082
{99,1,2}	1.0000	1.0000
{172,3,2}	1.0000	1.0000
{176,3,2}	1.0914	1.0027
{13,1,1}	1.0000	1.0000

6. Conclusion

This paper investigates centrality measures for multilayer networks by introducing the exponential and the resolvent of the adjacency tensor associated with this network using the Einstein product. We showed how to approximate these tensor functions via Krylov subspace methods based on the tensor format. Numerical tests gave satisfactory results. The paper illustrates the tensors are useful for modeling multilayer networks and can be used to evaluate small to quite large networks. However, the computations for very large networks and may require the use of parallel computers with many processors. This will be explored in future work.

Acknowledgment

The authors would like to thank the referees for comments that improved the presentation. Research by SN was partially supported by a grant from SAPIENZA Università di Roma and by INdAM-GNCS.

References

- [1] M. Al Mugahwi, O. De la Cruz Cabrera, and L. Reichel, Orthogonal expansion of network functions, *Vietnam J. Math.*, 48 (2020), pp. 941–962.
- [2] B. Beckermann and L. Reichel, Error estimation and evaluation of matrix functions via the Faber transform, *SIAM J. Numer. Anal.*, 47 (2009), pp. 3849–3883.
- [3] F. P. A. Beik, K. Jbilou, M. Najafi-Kalyani, and L. Reichel, Golub-Kahan bidiagonalization for ill-conditioned tensor equations with applications, *Numer. Algorithms*, 84 (2020), pp. 1535–1563.
- [4] A. Bentbib, M. El Ghomari, K. Jbilou, and L. Reichel, The Golub-Kahan method and Gauss quadrature for tensor function approximation, *Numer. Algorithms*, 92 (2023), pp. 5–34.
- [5] M. Benzi and C. Klymko, Total communicability as a centrality measure, *J. Complex Netw.*, 1 (2013), pp. 124–149.
- [6] K. Bergermann, Multiplex-matrix-function-centralities, <https://github.com/KBergermann/Multiplex-matrix-function-centralities>.
- [7] K. Bergermann and M. Stoll, Fast computation of matrix function-based centrality measures for layer-coupled multiplex networks, *Phys. Rev. E*, 105 (2022), Art. 034305.
- [8] R. Behera and D. Mishra, Further results on generalized inverses of tensors via the Einstein product, *Linear Multilinear Algebra*, 65 (2017), pp. 1662–1682.

- [9] L. Böttcher and M. A. Porter, Classical and quantum random-walk centrality measures in multilayer networks, *SIAM J. Appl. Math.*, 6 (2021), pp. 2704–2724.
- [10] M. Brazell, N. Li, C. Navasca, and C. Tamon, Solving multilinear systems via tensor inversion, *SIAM J. Matrix Anal. Appl.*, 34 (2013), pp. 542–570.
- [11] S. Cipolla, M. Redivo-Zaglia, and F. Tudisco, Shifted and extrapolated power methods for tensor ℓ^p -eigenpairs, *Electron. Trans. Numer. Anal.*, 53 (2020), pp. 1–27.
- [12] M. De Domenico, A. Solé-Ribalta, E. Cozzo, M. Kivelä, Y. Moreno, M. A. Porter, S. Gómez, and A. Arenas, Mathematical formulation of multilayer networks, *Phys. Rev. X*, 3 (2013), Art. 041022.
- [13] M. De Domenico, A. Solé-Ribalta, E. Omodei, S. Gómez, and A. Arenas, Centrality in interconnected multilayer networks, *arXiv:1311.2906v1*, (2013).
- [14] O. De la Cruz Cabrera, M. Matar, and L. Reichel, Analysis of directed networks via the matrix exponential, *J. Comput. Appl. Math.*, 355 (2019), pp. 182–192.
- [15] M. El Guide, A. El Ichi, F. P. Beik, and K. Jbilou, Tensor Krylov subspace methods via the Einstein product with applications to image and video processing, *Appl. Numer. Math.*, 181 (2022), pp. 347–363.
- [16] S. El-Halouy, S. Noschese, and L. Reichel, Perron communicability and sensitivity of multilayer networks, *Numer. Algorithms*, 92 (2023), pp. 597–617.
- [17] E. Estrada, Communicability geometry of multiplexes, *New J. Phys.*, 21 (2019), Art. 015004.
- [18] E. Estrada, *The Structure of Complex Networks: Theory and Applications*, Oxford University Press, Oxford, 2011.
- [19] E. Estrada and N. Hatano, Communicability in complex networks, *Phys. Rev. E*, 77 (2008), Art. 036111.
- [20] E. Estrada and D. J. Higham, Network properties revealed through matrix functions, *SIAM Rev.*, 52 (2010), pp. 696–714.
- [21] E. Estrada and J. A. Rodríguez-Velazquez, Subgraph centrality in complex networks, *Phys. Rev. E*, 71 (2005), Art. 056103.
- [22] C. Fenu, D. Martin, L. Reichel, and G. Rodríguez, Block Gauss and anti-Gauss quadrature with application to networks, *SIAM J. Matrix Anal. Appl.*, 34 (2013), pp. 1655–1684.

- [23] G. H. Golub and G. Meurant, *Matrices, Moments and Quadrature with Applications*, Princeton University Press, Princeton, 2010.
- [24] B. Huang, X. Yajun, and C. Ma, Krylov subspace methods to solve a class of tensor equations via the Einstein product, *Numer. Linear Algebra Appl.*, 26 (2019), Art. e2254.
- [25] K. Jbilou, A. Messaoudi, and H. Sadok, Global FOM and GMRES algorithms for matrix equations, *Appl. Numer. Math.*, 31 (1999), pp. 49–63.
- [26] K. Jbilou, H. Sadok, and A. Tinzeft, Oblique projection methods for multiple linear systems, *Electron. Trans. Numer. Anal.*, 20 (2005), pp. 119–138.
- [27] L. Katz. A new status index derived from sociometric analysis, *Psychometrika*, 18 (1953), pp. 39–43.
- [28] T. G. Kolda and B. W. Bader, *MATLAB tensor toolbox*, Sandia National Laboratories (SNL), Albuquerque, NM, and Livermore, CA, 2006.
- [29] T. G. Kolda and B. W. Bader, Tensor decompositions and applications, *SIAM Rev.*, 51 (2009), pp. 455–500.
- [30] M. Kivelä, A. Arenas, M. Barthelemy, J. P. Gleeson, Y. Moreno, and M. A. Porter, Multilayer networks, *J. Complex Netw.*, 2 (2014), pp. 203–271.
- [31] K. Lund, The tensor t-function: A definition for functions of third-order tensors, *Numer. Linear Algebra Appl.*, 27 (2020), Art. e2288.
- [32] F. McGee, M. Ghoniem, G. Melançon, B. Otjacques and B. Pinaud, The state of the art in multilayer network visualization, *Computer Graphics Forum*, 38 (2019), pp. 125–149).
- [33] L. Qi and Z. Luo, *Tensor Analysis: Spectral Theory and Special Tensors*, SIAM, Philadelphia, 2017.
- [34] D. Taylor, M. A. Porter, and P. J. Mucha, Tunable eigenvector-based centralities for multiplex and temporal networks, *Multiscale Model. Simul.*, 19 (2021), pp. 113–147.
- [35] M. Wu, S. He, Y. Zhang, J. Chen, Y. Sun, Y. Liu, J. Zhang, and H. V. Poor, A tensor-based framework for studying eigenvector multicentrality in multilayer networks, *Proc. NAS*, 116 (2019), pp. 15407–15413.